Pair potentials on metal surfaces

Mark Rasolt
Solid State Division, Oak Ridge National Laboratory, Oak Ridge, Tennessee 37830

F. Perrot
Commissariat à l'Energie Atomique, Boîte Postale 27, F-94190 Villeneuve-Saint-Georges, France
(Received 13 September 1982; revised manuscript received 21 June 1983)

A model representation of a simple metal surface was used to calculate pair potentials between atoms, both inside and outside the surface region, which are then solved *exactly* in the random-phase approximation. Various lattice planes and atomic configurations are considered, and features which are independent of the detail of the model are extracted.

I. INTRODUCTION

Consider a collection of ions positioned at points $\{\vec{R}_i\}$ and surrounded by a neutralizing electron charge of density $n(\vec{r})$. An infinitesimal displacement of an ion at point $\vec{R}_1$ introduces a perturbing potential $\delta V_1(\vec{r}-\vec{R}_1)$ and an energy change given rigorously[1] by

$$\Delta E=-\tfrac{1}{2}\sum_{\vec{R}_i,\vec{R}_j}\int d^3r\int d^3r'\delta V_i(\vec{r}-\vec{R}_i)\chi(\vec{r},\vec{r}')\times\delta V_j(\vec{r}'-\vec{R}_j)\,, \tag{1}$$

where $\chi(\vec{r},\vec{r}')$ is the electronic response function appropriate to the density $n(\vec{r})$. Equation (1) is thus the core of the calculation of bulk phonons,[2] bulk-phonon softening,[3] pair interactions in liquid metals,[4] surface phonons,[5] surface reconstruction,[5,6] and more.

The changes in χ, by going from bulk to surface properties, has been particularly interesting. The effect of charge redistribution (in the surface region) on the surface-phonon density of states has been estimated within a very simple model.[7] Approximate structures of χ (which include such charge transfer corrections) have been employed in surface tension, surface-phonon, and surface energy calculations.[8–10] Surface reconstruction in semiconductors as well as metals has been attributed to changes in $\chi(\vec{r},\vec{r}')$ both at temperature $T=0$ and finite T. Although such effects (in χ) have been assigned to surface states,[5,6] and their corresponding Fermi-surface nesting properties[11] (smeared at higher T), the upshot is always a change in the force constants in Eq. (1).[5] Since even the more complicated metal surfaces contain a large component (in χ) of *s-p* electrons, the effect of simple charge transfer (at the surface) must play a major role in all of the above properties (persisting even to high T); it is this which we want to study here. As a first step in that direction we evaluate Eq. (1) *exactly* for a well-defined model and in the process provide *exact* results for comparison with previous approximations of χ, and draw trends and order-of-magnitude estimates of the changes in the surface pair potential (both inside and outside the surface region) which are likely to be insensitive to the choice of the model.

In Sec. II we set up our solution of Eq. (1) for a jellium profile. In Sec. III we generate the pair interaction of two ions outside and inside the metal surface region. These results are discussed in Sec. IV.

Finally, we note that the response of more realistic metal surfaces do indeed exist.[12] However, such calculations have been largely restricted to perturbations with no variation parallel to the metal surface. As we shall see in Sec. II, the construction of pair interactions requires the detailed response for a range of wave vectors necessary to reproduce the important asymptotic Friedel oscillations in the pair potentials. To our knowledge, no such calculations exist for any model of a simple metal surface and certainly not for a "real" surface profile.[10]

II. PAIR INTERACTIONS AT A JELLIUM SURFACE; FORMULATION

If we consider an arbitrary external potential $V(\vec{r})$ and a set of auxiliary wave functions $\phi_{\vec{k}}(\vec{r})$, then according to Kohn and Sham[13] the ground-state density $n(\vec{r})$ is given by

$$n(\vec{r})=\sum_{\vec{k}}^{\text{occ}}\phi^*_{\vec{k}}(\vec{r})\phi_{\vec{k}}(\vec{r})$$

and the $\phi_{\vec{k}}(\vec{r})$ satisfy

$$\left[-\frac{\hbar^2}{2m}\nabla^2+V_{\text{eff}}(\vec{r})\right]\phi_{\vec{k}}(\vec{r})=\epsilon_{\vec{k}}\phi_{\vec{k}}(\vec{r})\,, \tag{2}$$

where

$$V_{\text{eff}}(\vec{r})=V(\vec{r})+V_H(n(\vec{r}))+v_{\text{xc}}(n(\vec{r}))$$

with $V_H(n(\vec{r}))$ and $v_{\text{xc}}(n(\vec{r}))$ the usual Hartree and exchange-correlation potentials which are functionals of $n(\vec{r})$. The longitudinal susceptibility $\chi(\vec{r},\vec{r}')$ [of Eq. (1)] is given rigorously[14] as a solution of

$$\chi(\vec{r},\vec{r}')=\Pi(\vec{r},\vec{r}') - \int d^3r'' \int d^3r'''\Pi(\vec{r},\vec{r}'') \times v(\vec{r}''-\vec{r}''')\chi(\vec{r}''',\vec{r}') , \quad (3)$$

with $v(\vec{r}-\vec{r}')=e^2/|\vec{r}-\vec{r}'|$ and where Π is the irreducible response function (see Fig. 1); the propagators are all constructed from the $\phi_{\vec{k}}(\vec{r})$ in the usual way, i.e.,

$$G(\vec{r},\vec{r}')=\sum_{\vec{k}} \phi^*_{\vec{k}}(\vec{r})\phi_{\vec{k}}(\vec{r}')[\omega-\epsilon_{\vec{k}}+i\delta\,\mathrm{sgn}(\omega-\mu)]^{-1}$$

and μ is the noninteracting chemical potential.

For a jellium surface the translational symmetry along the surface reduces Eq. (3) to

$$\chi(q_{||},z,z')=\Pi(q_{||},z,z')- \int dz'' \int dz'''\Pi(q_{||},z,z'') \times v(q_{||},z'',z''') \times\chi(q_{||},z''',z') , \quad (4)$$

where, e.g.,

$$\chi(\vec{q}_{||},z,z')= \int d^2\rho\, e^{i\vec{q}_{||}\cdot\vec{\rho}}\chi(\vec{\rho},z,z')$$

(z and z' are perpendicular to the surface). The electrons are confined between two imaginary surfaces separated by a distance L (the jellium background is bounded by these imaginary surfaces and separated by some arbitrary microscopic distance from them) then it is useful to write Eq. (4) in cosine transform, i.e.,

$$\chi(q_{||},z,z')= \sum_{q,q'} \cos(qz)\cos(q'z')\chi(q_{||},q,q') , \quad (5a)$$

where q and $q'=n\pi/L$, $n=0\pm1,\pm2,\pm3,\ldots$, and

$$\chi(q_{||},q,q')=\frac{1}{L^2}\int_0^L dz \int_0^L dz'\cos(qz)\cos(q'z')\chi(q_{||},z,z') , \quad (5b)$$

then Eq. (4) becomes

$$\chi(q_{||},q,q')=\Pi(q_{||},q,q')- \sum_{q'',q'''} \Pi(q_{||},q,q'') \times v(q_{||},q'',q''')\chi(q_{||},q''',q), \quad (6)$$

where

$$v(q_{||},q,q')=\frac{L2\pi e^2}{q^2+q_{||}^2}(\delta_{q,-q'}+\delta_{q,q'}) - \frac{4\pi e^2 q_{||}}{(q^2+q_{||}^2)(q'^2+q_{||}^2)} , \quad (7)$$

where both q and q' are either even or odd (zero otherwise). Equation (1), for *one* pair interaction between an ion at $\vec{R}_1$ and a second ion at $\vec{R}_2$ can now be written as

$$\Delta E_{12}\equiv\Phi=\frac{1}{2\pi}\int_0^\infty dq_{||}q_{||}J_0(q_{||}\rho)F(q_{||},z_1,z_2) , \quad (8)$$

where $|\vec{R}_1-\vec{R}_2|=[\rho^2+(z_1-z_2)^2]^{1/2}$, $J_0(q_{||}\rho)$ is the cylindrical Bessel function, and

$$F(q_{||},z_1,z_2)=L^2\sum_{q,q'}\delta V_1(q_{||},q,z_1)\chi(q_{||},q,q') \times\delta V_2(q_{||},q',z_2) . \quad (9)$$

The form of Eq. (6) is unfortunately not very suitable for numerical solution which proceeds best by successive iteration. Such an iterative solution closely resembles a sum of an expansion in powers of $v(q_{||},q'',q''')$. Gell-Mann and Brueckner[15] (for example) pointed out the error in such an expansion and showed that the correct interparticle interaction *must* be $4\pi e^2/[Q^2\epsilon(Q)]$ $[Q\equiv(q_{||}^2+q^2)^{1/2}]$ where

$$\epsilon(Q)=1+\frac{4\pi e^2}{Q^2}\Pi_B(Q)$$

(the bulk dielectric function).[16] We therefore cast Eq. (6) in such a form following Ref. 17, i.e., if a surface did not exist, then

$$\Pi(q_{||},q,q')=\frac{\Pi_B(Q)}{L}\delta_{q,q'} .$$

The effect of the surface is to introduce a nondiagonal correction $\psi^0(q_{||},q,q')$, so that

$$\Pi(q_{||},q,q')=\frac{\Pi_B(Q)}{L}\delta_{q,q'}+\psi^0(q_{||},q,q') . \quad (10)$$

We define the function $\tilde{\chi}(q_{||},q,q')$ such that χ of Eq. (6) is written as

$$\chi(q_{||},q,q')=\tilde{\chi}(q_{||},q,q')- \sum_{q'',q'''}{}' \chi(q_{||},q,q'')\frac{4\pi e^2 q_{||}}{(q_{||}^2+q''^2)(q_{||}^2+q'''^2)}\tilde{\chi}(q_{||},q''',q') , \quad (11)$$

where the prime over the summation sign restricts q'' and q''' to both even or odd. With simple matrix manipulation Eq. (4) for χ can be transformed to an equation for $\tilde{\chi}$, i.e.,

$$\tilde{\chi}(q_{||},q,q')=\frac{\Pi_B(Q)}{L}\delta_{q,q'}-L\sum_{q''}\Pi(q_{||},q,q'')\frac{4\pi e^2}{q_{||}^2+q''^2}\tilde{\chi}(q_{||},q'',q') . \quad (12)$$

Finally, we define[17]

$$\tilde{\chi}(q_{||},q,q')=\frac{\Pi_B(Q)}{L\epsilon(Q)}\delta_{q,q'}+\frac{\psi(q_{||},q,q')}{\epsilon(Q)\epsilon(Q')} \quad [Q'=(q_{||}^2+q'^2)^{1/2}] . \quad (13)$$

The integral equation (12) can be rewritten only for the surface corrections,

$$\psi(q_{||},q,q')=\psi^0(q_{||},q,q')-L\sum_{q''}\psi^0(q_{||},q,q'')\frac{4\pi e^2\psi(q_{||},q'',q')}{(Q'')^2\epsilon(Q'')}\ ,$$

where (14)

$$Q''=(q_{||}^2+q''^2)^{1/2}\ ,$$

and the iteration of Eq. (14) now proceeds in terms of only the *screened* interparticle interaction. The $\chi(q_{||},q,q')$ of Eq. (11) is then given by solving Eq. (14) numerically for ψ (when ψ^0 is known; see the following sections). By back tracking to Eq. (13) we get $\tilde{\chi}$, and from Eq. (11) χ is analytically solvable due to the separability of the kernel.

We conclude by listing the full form of Eq. (9) (i.e., of Φ). We write

$$F(q_{||},z_1,z_2)=A(q_{||},z_1,z_2)+B(q_{||},z_1,z_2)+C(q_{||},z_1,z_2)+D(q_{||},z_1,z_2)+E(q_{||},z_1,z_2)\ , \tag{15}$$

where

$$A(q_{||},z_1,z_2)=-L\sum_{q}\delta V_1(q_{||},q,z_1)\frac{\Pi_B(Q)}{\epsilon(Q)}\delta V_2(q_{||},q,z_2)\ , \tag{16a}$$

$$B(q_{||},z_1,z_2)=-\sum_{q,q'}\delta V_1(q_{||},q,z_1)\frac{\psi(q_{||},q,q')}{\epsilon(Q)\epsilon(Q')}\delta V_2(q_{||},q',z_2)\ , \tag{16b}$$

$$C(q_{||},z_1,z_2)=-\frac{q_{||}}{8\pi D(q_{||})}\sum_{q,q'}\left[\frac{\delta V_1(q_{||},q,z_1)\Pi_B(Q)4\pi e^2}{Q^2\epsilon(Q)}\right]\left[\frac{\delta V_2(q_{||},q',z_2)\Pi_B(Q')4\pi e^2}{Q'^2\epsilon(Q')}\right]\ , \tag{16c}$$

$$D(q_{||},z_1,z_2)=-\frac{1}{8\pi}\frac{q_{||}L}{D(q_{||})}\sum_{q,q',q''}\left[\left[\frac{\delta V_1(q_{||},q,z_1)\Pi_B(Q)4\pi e^2}{Q^2\epsilon(Q)}\right]\times\left[\frac{\delta V_2(q_{||},q'',z_2)\psi(q_{||},q',q'')4\pi e^2}{Q'^2\epsilon(Q')\epsilon(Q'')}\right]+(\delta V_1\leftrightarrow\delta V_2)\right]\ , \tag{16d}$$

$$E(q_{||},z_1,z_2)=-\frac{1}{8\pi}\frac{q_{||}L^2}{D(q_{||})}\left[\left[\sum_{q,q'}\frac{\delta V_1(q_{||},q',z_1)\psi(q_{||},q,q')4\pi e^2}{Q^2\epsilon(Q)\epsilon(Q')}\right]\left[\sum_{q,q'}\frac{\delta V_2(q_{||},q',z_2)\psi(q_{||},q,q')4\pi e^2}{Q^2\epsilon(Q)\epsilon(Q')}\right]\right]\ . \tag{16e}$$

In Eqs. (16c)—(16e) $D(q_{||})$ is given by

$$D(q_{||})=1-\frac{q_{||}}{8\pi L}\sum_{q}\frac{\Pi_B(Q)}{\epsilon(Q)}\left[\frac{4\pi e^2}{Q^2}\right]^2-\frac{q_{||}}{8\pi}\sum_{q,q'}\frac{\psi(q_{||},q,q')(4\pi e^2)^2}{\epsilon(Q)\epsilon(Q')Q^2Q'^2}\ . \tag{17}$$

We now note the difference between the solution of Eq. (14) for a nonvarying external perturbation parallel to the surface[12] and that required for pair interactions. The latter is a much lower symmetry problem which requires a detailed numerical study of Eq. (14) in the region of $(q_{||}^2+q^2)\cong(q_{||}^2+q'^2)\cong 4k_F^2$ to reproduce properly the important Friedel oscillations.

In the following section we solve Eq. (14) *exactly* for a model surface and evaluate Eqs. (8), (9), and (16) *exactly* for a variety of pair-potential configurations.

III. NUMERICAL RESULTS

A. The model

We choose for the description of the surface the infinite-barrier model (IBM). It is worth making a few comments concerning self-consistency as described in Eq. (2). The IBM *does not* mean that the external potential of the positive jellium is represented by $V(z)=\lambda\Theta^>(z)$ [$\lambda\rightarrow\infty$ $\Theta^>(z)=1$ when $z>0$, and $\Theta^>(z)=0$ when $z<0$]; actually $\lambda\Theta^>(z)$ corresponds to $V_{\rm eff}$. The *external potential* $V(z)$ is equal to

$$V(z)=V_{\rm eff}(z)-V_H(n(z))-v_{\rm xc}((z))\ . \tag{18}$$

The density $n(z)$ is constructed from the $\phi_{\vec{k}}(\vec{r})$ which are solutions to $\lambda\Theta^>(z)$. In this way we have developed fully self-consistent wave functions and density appropriate to the *external* potential given in Eq. (18).

To evaluate the appropriate form for $\psi^0(q_{||},q,q')$ in Eq. (10) (neglecting correlations for the moment) we evaluate the first bubble graph of Fig. 1 using in $G(\vec{r},\vec{r}')$, $\phi_{\vec{k}}(\vec{r})=\sin(k_z z)e^{i\vec{k}_{||}\cdot\vec{\rho}}/[(L/2)^{1/2}A^{1/2}]$ (A is the surface area). Taking the

cosine transforms according to Eq. (5b) yields the following results for the static $\psi^0(q_{||},q,q')$:

$$\psi^0(q_{||},q,q')=+\frac{m}{\hbar^2\pi 4L^2q_{||}^2}\frac{q_{||}^2-qq'}{|q_{||}^2-q'q|}[(q_{||}^2-q'q)^2-4k_F^2q_{||}^2+(q+q')^2q_{||}^2]^{1/2}[1-\Theta^>((q+q')^2-4k_F^2)] \tag{19a}$$

when the function in the square root is positive and

$$\psi^0(q_{||},q,q')=-\frac{m}{\hbar^2\pi 4L^2q_{||}^2}(q_{||}^2-qq')[1-\Theta^>((q+q')^2-4k_F^2)] \tag{19b}$$

when the function in the square root is negative. It is not difficult to show that in Eq. (19)

$$\frac{\pi}{L}\sum_{q'}\psi^0(q_{||},q,q')=-\Pi_B^0(Q)\ , \tag{20}$$

where Π_B^0 is the uncorrelated (Lindhard) screening function.

B. Pair potentials outside the surface

We now place the two ions outside the surface, a distance z_1 from the terminating L (i.e., one of the imaginary planes surrounding the jellium background) and separated by a distance $\vec{\rho}$ parallel to the surface. No matter what the pseudopotential choice for the two ions (see below), when z_1 is outside the surface and bigger than the core radius R_c (see below) δV in Eq. (9) becomes that of a point charge. That is,

$$\delta V_1(q_{||},q,z_1)=-\frac{2\pi Ze}{LQ^2}e^{-q_{||}z_1}\ , \tag{21}$$

where Z is the valence of the ions (we take $Z=3$ and an electron density n_0 insider the IBM [i.e., $(4\pi/3)r_s^3=1/n_0$; $r_s=2.07$], both corresponding to aluminum).

By far the greatest difficulty of evaluating Eqs. (9) and (16) is the solution of the integral equation [Eq. (14)]. It demands a very accurate numerical result around $(q_{||}^2+q^2)\cong 4k_F^2$ to properly pick up the expected weak logarithmic singularities (which are well known to exist in the bulk contributions) which govern the asymptotic behavior of the pair potential. We therefore *do not* solve it for the full susceptibility. From Eqs. (16b), (16d), (16e) and (17) we note that only related quantities such as

$$\sum_{q'}\delta V_1(q_{||},q',z_1)\psi(q_{||},q,q')/\epsilon(Q')$$

or

$$\sum_{q'}4\pi e^2\psi(q_{||},q,q')/[Q'^2\epsilon(Q')]$$

are required. [In other words Eq. (14) can be cast as a vector equation rather than the matrix equation for the full ψ.] We achieve an iterative solution of Eq. (14) to an accuracy of better than 10^{-3} for the full range of $q_{||}$ and q. The IBM, however, provides, in addition, a test in that at the surface boundary L (or equivalently $z=0$) the induced density (due to δV_1) *must be* zero. It is an obvious consequence of the density $n_0(z)$ (in the IBM) going identically to zero at $z=0$, i.e.,

$$n_0(z)=n_0[1+3/y^3(y\cos y-\sin y)]\ , \tag{22}$$

with $y=2k_Fz$.

The induced density along z (averaged along $\vec{\rho}$) is given by

$$n_1(z)=-\lim_{q_{||}\to 0}L^2\sum_{q,q'}\cos(qz)\chi(q_{||},q,q')\delta V_1(q_{||},q',z_1)\ . \tag{23}$$

We can easily cast Eq. (23) in terms of $\psi(q_{||},q,q')$ following the derivation of Eq. (16) and the resulting structure is very similar (it will not be detailed here).

Our results for $n_1(z)$ (neglecting correlation) are presented in Fig. 2. More precisely, in Eq. (14) we use the ψ^0 of Eq. (19) and the Lindhard dielectric function is used for $\epsilon(Q)$ in both Eqs. (14) and (16).

It has been long recognized that the effect of correlations in the response function of the uniform system adds major modifications to the induced density and the corresponding pair potential.[16] There is no reason to believe that similar effects will not occur at a metal surface. To include such many-body corrections at a metal surface is manyfold more complicated, due to the surface nonuniformity. In other words, to include exchange and correlation in Eqs. (14) and (16) requires the *same* level of approxima-

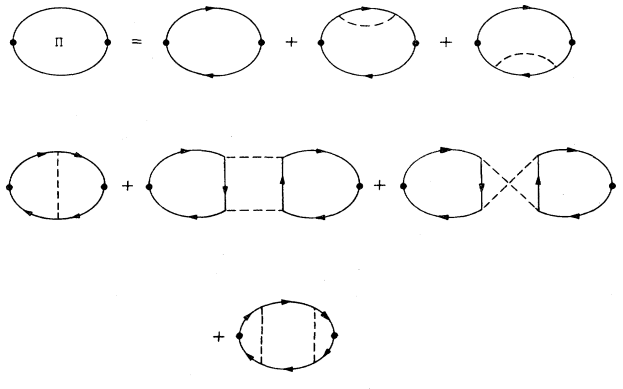

FIG. 1. Low-order screening functions. Graphs included in $\Pi_B(Q)$ are the Lindhard first five lowest-order and one example of higher-order RPA. Dashed lines are actually dynamically screened interactions.

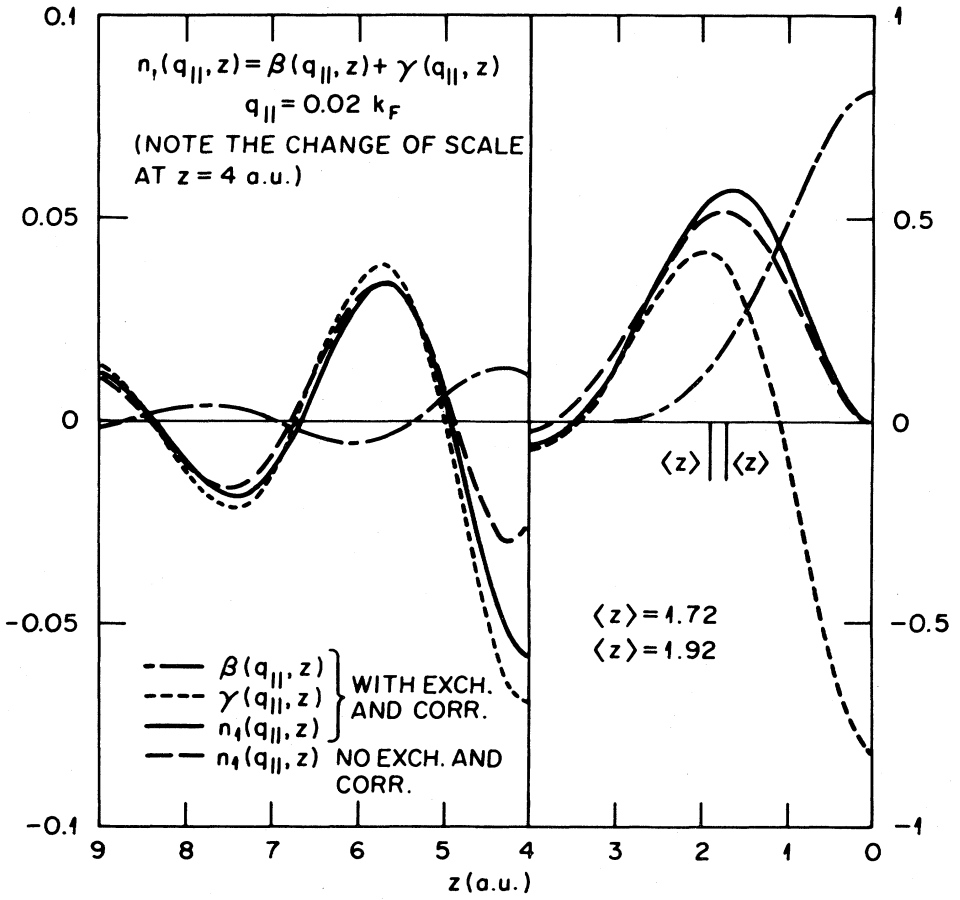

FIG. 2. Induced charge density (averaged along the surface) in the IBM for a positive point charge of $Z=1$ located outside the metal surface. $\beta(q_{||},z)$ is the contribution within the semiclassical approximation. $\gamma(q_{||},z)$ is the contribution from the quantum interference (or equivalently the fine detail of the surface). Two densities with and without exchange and correlation are included for a substrate density of Al ($r_s=2.07$). Location of the image plane is labeled by $\langle z\rangle$ and the $\langle z\rangle=1.92$ includes no exchange correlation while $\langle z\rangle=1.72$ does. Note that our convention labels z always positive whether in or out of the solid and is the distance from the IBM boundary at L.

tion for $\psi^0(q_{||},q,q')$ as the one entering the uniform correlated $\Pi_B(Q)$. Consider Fig. 1; if we include this series of graphs in $\Pi_B(Q)$ we must extract the form of $\psi^0(q_{||},q,q')$ for the same set of terms; in other words we calculate these graphs with the propagator constructed out of the IBM wave function (see above), but that is clearly unaccessible. In fact it is further complicated since the interparticle interaction must be properly screened (see above, now dynamically). We take the following simplified approach. (1) We borrow the algorithm of Hubbard[18] and introduce higher-order corrections via a similar enhancement factor. (2) We ensure that our approximation satisfies the sum rule of the IBM [i.e., that $n_1(z=0)=0$]. We can verify that the transformation,

$$\psi^0(q_{||},q,q')\rightarrow\psi^0(q_{||},q,q')\Pi_B(Q')/\Pi_B^0(Q')\ , \tag{24}$$

is appropriate [this is guided by Eq. (20)]; of course, the dielectric function $\epsilon(Q)$ is now also $1+4\pi e^2/q^2\Pi_B(Q)$.

At first sight it seems that in Eq. (24) we have violated the symmetry between q and q' in $\chi(q_{||},q,q')$. Remember, however, that we are not really interested in χ itself but in various sums over q and q'. Equation (24) is an alogorithm for including exchange and correlation in the pair potentials *and not* for providing the full form of χ.

In Fig. 2 we include the effect of correlation in the induced charge $n_1(z)$. The corresponding interaction of a point charge with the surface is displayed in Fig. 3, and the corresponding pair interactions are detailed in Fig. 4. These results are discussed in the following section.

C. Pair potentials inside the surface

The calculation of pair potentials inside the surface region differs only in the form for $\delta V_1(q_{||},q,z')$, since now the explusion of the electrons from the core region R_c must be included. For Al we use a local Heine-Abarenkov pseudopotential $\delta V_1(\vec{r})$,

$$\delta V_1(\vec{r})=\frac{-ZD}{R_c}[1-\Theta^>(r-R_c)]-\frac{Ze}{r}\Theta^>(r-R_c)\ .$$

It is not difficult to calculate the cosine transform of $\delta V_1(\vec{r})$; it is

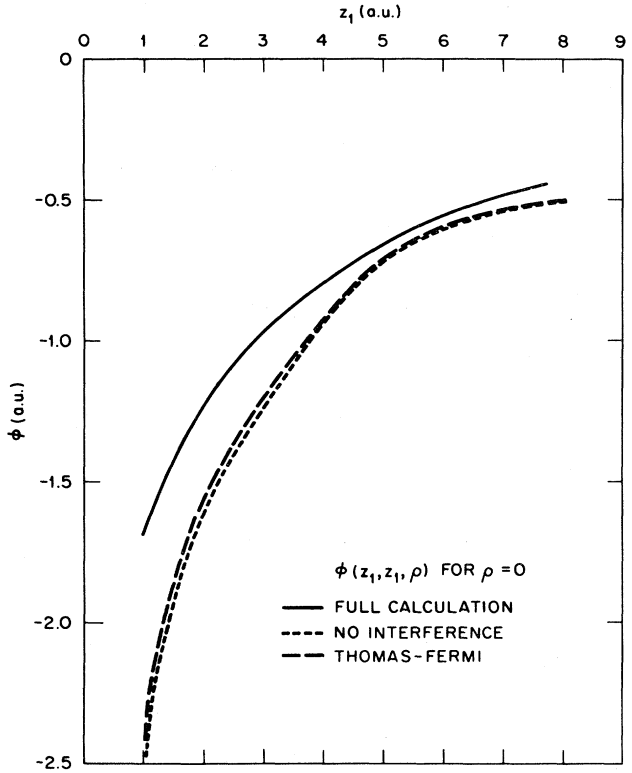

FIG. 3. Potential surface of a point charge of $Z=3$ outside the metal surface. Full calculation [Eq. (16)] includes the effects of exchange and correlation (see text); same for the SCA [i.e., no interference $\psi=0$ in Eq. (16)]. Thomas-Fermi approximation sets $\psi=0$ and $\epsilon(Q)$ to the TF approximation in Eq. (16).

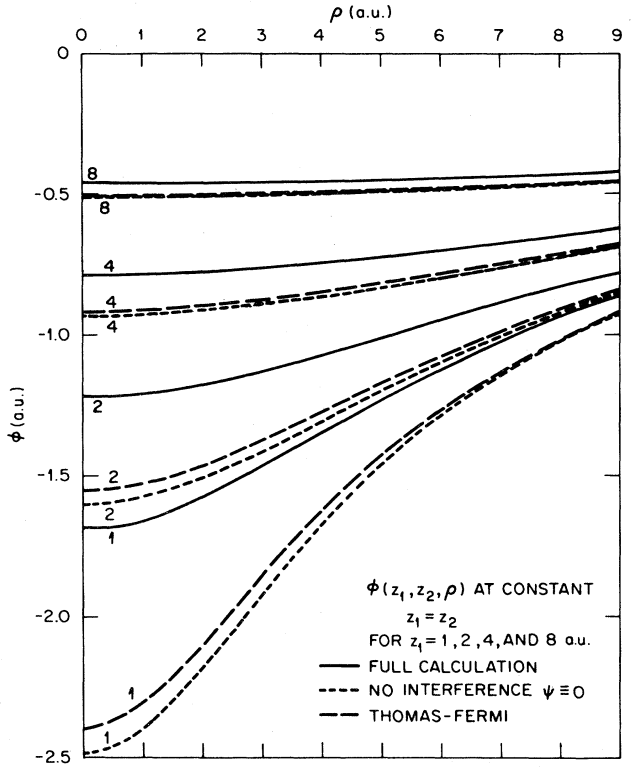

FIG. 4. Pair interactions outside the metal surface for two ions (of $Z=3$) at various positions z_1 away from the surface and as a function of their separation ρ. Note that the bare repulsion (ϕ_{bare} in text) is not included.

$$\delta V_1(q_{||},q,z_1)=-\frac{2\pi Ze}{LQ^2}\left[-2\cos(qz_1)\left[\frac{D\sin(QR_c)}{QR_c}+(1-D)\cos(QR_c)\right]+e^{-q_{||}z_1}\right]. \tag{25}$$

The parameters D and R_c have been determined in the spirit of Ref. 19 by matching a full self-consistent charge density (see Fig. 5). However, the IBM cannot account for the microscopic electron-density variation (e.g., an Al surface), and we do not imply that the following results are a detailed account of the corresponding pair interactions for a real Al surface.

In Fig. 6 we present the structure of $F(q_{||},z_1,z_1)$ [note that the bulk contribution to ϕ, $-\frac{1}{2}\delta V_1(Q,z_1)\Pi_B(Q)\delta V_1(Q,z_1)/\epsilon(Q)$, has been removed] for the full range of $q_{||}$ with and without exchange and correlation. Figure 7 depicts the rate of convergence of the surface contribution ϕ_s for three planes inside the surface region. Figures 8—10 display the surface correction to ϕ for various planes and configurations of the pair interactions. We turn to these results next.

IV. DISCUSSION

In the preceding section we presented pair potentials which are *exact* within the random-phase approximation (RPA) for a metal jellium surface described by an external

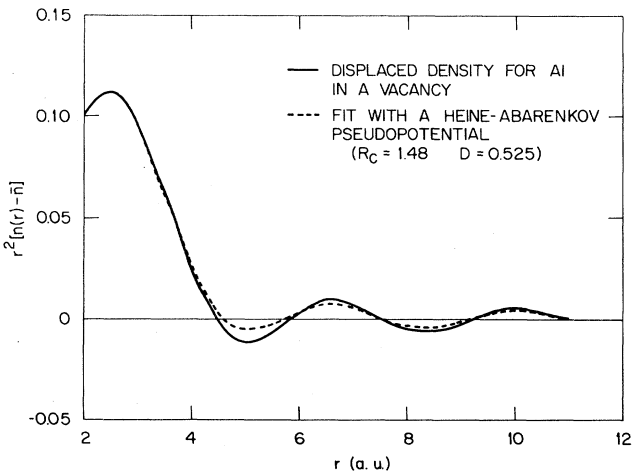

FIG. 5. Solid curve is the full self-consistent screening density for an aluminum ion placed in a vacancy of a jellium (Ref. 19) of $r_s=2.07$. Dashed curve is the best fit we could achieve using a local Heine-Abarenkov potential of well depth $D=0.525$ and core radius $R_c=1.48$ a.u.

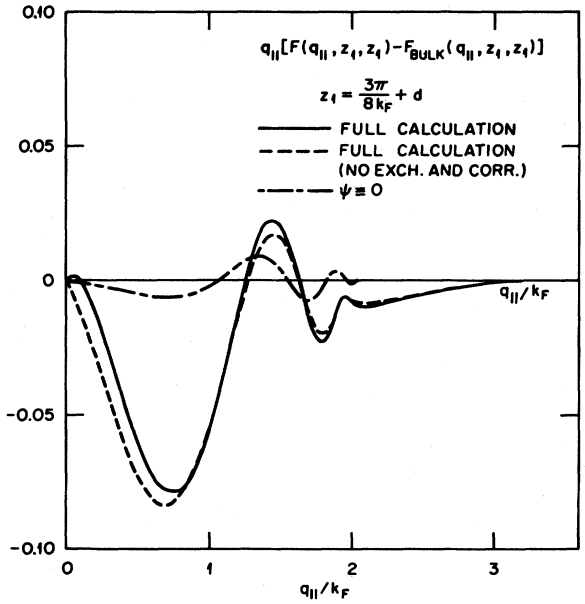

FIG. 6. Detailed behavior of the surface contribution to $F(q_{||},z_1,z_2)$ [using the pseudopotential of Eq. (25)] as a function of $q_{||}$ [entering Eq. (8)] for the two ions placed in the second plane of a (110) face of Al. Effect of exchange and correlation (solid curve) is of particular interest.

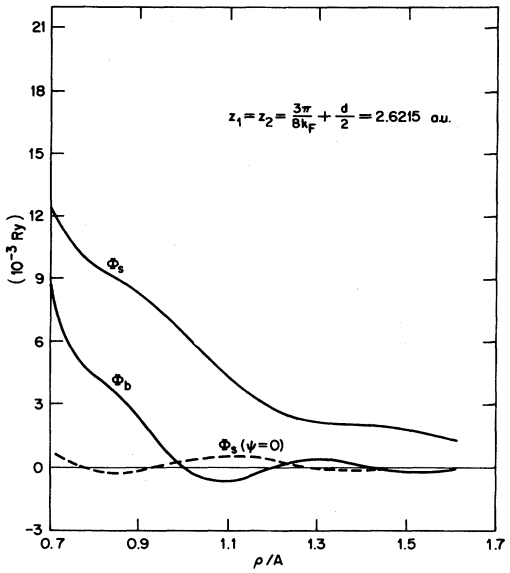

FIG. 8. Surface contribution ϕ_s (to the bulk pair interaction ϕ_b) for two Al pseudo ions in the first plane of a (110) face of Al as a function of their separation ρ. Dashed curve is SCA. Exchange and correlation are included as discussed in text. Note that ϕ_b does include the repulsion of the two ions ϕ_{bare}.

potential given in Eq. (18) and corresponding density of Eq. (22). The fine details of the IBM certainly present many variances with a realistic jellium profile.[20–26] The solution of Eqs. (8), (9) and (16) for a real jellium profile with the required accuracy around $2k_F$ (see above) is extremely difficult and has not as yet been carried out. When such a solution is available it must, however, reduce to the above results in the IBM limit. In addition, the exact pair potentials (presented here) are important in assessing the variety of approximations previously used to mimic the presence of the metal surface. The most common approximation is

$$\phi \approx -\tfrac{1}{2}\int d^3r \int d^3r' \delta V_1(\vec{r}-\vec{R}_1) \times \chi_B\left[\vec{r}-\vec{r}', \frac{n_0(\vec{r})+n_0(\vec{r}')}{2}\right] \times \delta V_2(\vec{r}'-\vec{R}_2)\,. \tag{26}$$

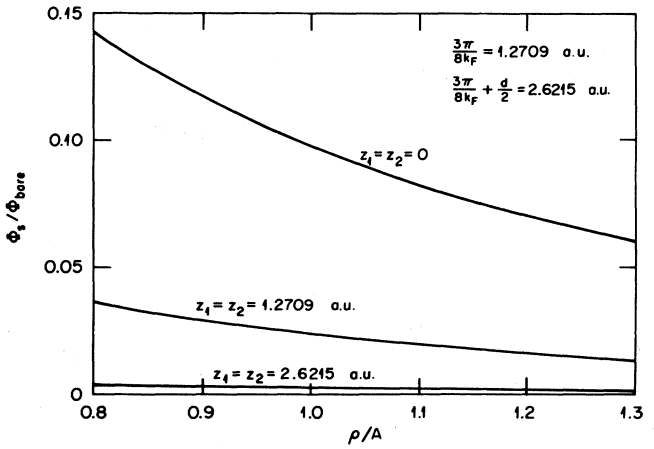

FIG. 7. Rate of convergence of ϕ_s vs ϕ_{bare} (see text) for two Al pseudo ions [Eq. (25)] placed on three planes and as a function of their separation ρ (A is the lattice constant of Al).

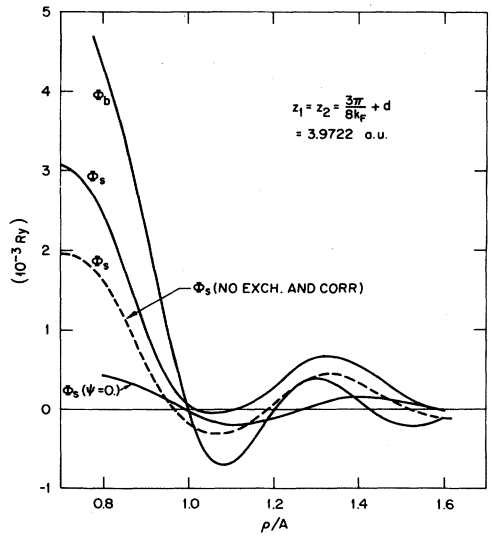

FIG. 9. Same as Fig. 8 for the second plane of a (110) face of Al. We inserted, also, the surface contribution without exchange and correlation in dashed curve.

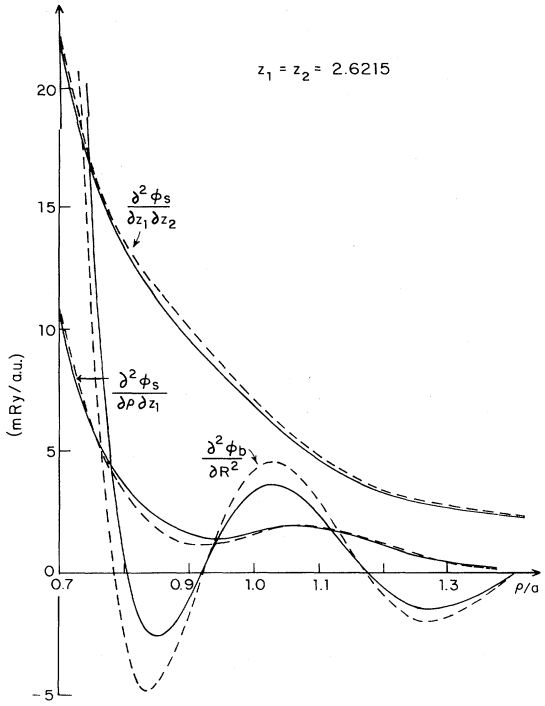

FIG. 10. Second derivatives of ϕ_s and ϕ_b. Perpendicular force constants to the surface are related to $\partial^2\phi_s/\partial z_1\partial z_2$ and the force constants coupling vibration parallel and perpendicular to the surface are related to $\partial^2\phi_s/\partial\rho\,\partial z_1$. Solid curves correspond to pseudopotential parameters $R_c=1.48$ and $D=0.525$, and the dashed curves to $R_c=1.386$ and $D=0.3969$.

Equation (26) is an extension of the local density approximation[13] (LDA) which similarly assigns a local density variation in the bulk susceptibility of the uniform electron gas. However, Eq. (26) is clearly much more demanding than the LDA for one-electron potentials.[13] Our preliminary results, using Eq. (22) in Eq. (26), cast doubts as to its value in surface pair-potential calculations.

We next return to our results in Figs. 2—10. These provide the following interesting features of a metal surface which are very likely to survive in a real metal surface. (1) The extent to which the Thomas-Fermi (TF) or semiclassical approximation [SCA, only Eqs. (16a) and (16c)] gives an adequate description for ϕ outside the metal surface. (2) The rate of approach ($z_1\rightarrow\infty$) to the image potential form and the position of the image plane. (3) Rate of convergence to the bulk pair potentials for different planes in the bulk. (4) Qualitative changes in the structure of the pair potentials; in particular, shifts in the positions of the minima. (5) Structure of pair potential in terms of different planes. (6) Effects of exchange and correlation on the pair potentials. From Fig. 2 we first observe the accuracy of our numerical results by noting the extent that $n_1(z=0)=0$. The limit $q_{||}\rightarrow 0$ was adequately achieved by setting $q_{||}=0.02k_F$ [note that in this figure we used $Z=1$ (not $Z=3$) in Eq. (21)]. $\beta(q_{||},z)$ represents the induced density in the SCA and $\gamma(q_{||},z)$ is the quantum interference corrections (due to ψ). Most interesting is the importance of exchange and correlation [particularly in the long-range oscillations of $n_1(z)$] and the range of the oscillations [in $n_1(z)$] very deep into the solid. The position of the image plane $\langle z\rangle$, defined as

$$\lim_{\rho\rightarrow 0}\phi(z_1,z_2,\rho)=\lim_{\rho\rightarrow 0}\frac{-Z^2e^2}{[(z_1+z_2+2\langle z\rangle)^2+\rho^2]^{1/2}} \tag{27}$$

is also inserted in Fig. 2. By using Eq. (16) we can readily show that

$$\langle z\rangle=\lim_{q_{||}\rightarrow 0}\left[\frac{1}{q_{||}}-\frac{1}{L}\sum_q\frac{4\pi e^2}{Q^4}\frac{\Pi_B(Q)}{\epsilon(Q)}-\sum_{q,q'}\frac{4\pi e^2}{Q^2Q'^2}\frac{\psi(q_{||},q,q')}{\epsilon(Q)\epsilon(Q')}\right]. \tag{28}$$

From Fig. 2 the effect of exchange and correlation on $\langle z\rangle$ is clearly non-negligible. From Figs. 3 and 4 we discover (as expected) that the pair interactions are adequately represented (to within 5%) by an image potential form of Eq. (27) (down to $z_1=1$) shifted by the appropriate $\langle z\rangle$.

Figure 7 shows the rate of convergence of the surface contribution ϕ_s (inside the surface region) relative to the bare interaction

$$\phi_{\text{bare}}\equiv+Z^2e^2/|\vec{R}_1-\vec{R}_2|\ .$$

ϕ_s is *only* the surface contribution to Eqs. (9) and (16). In other words, the usual electronic contribution ϕ_e, i.e.,

$$\phi_e=-\frac{1}{2}\int\frac{d^3Q}{(2\pi)^3}e^{i\vec{Q}\cdot(\vec{R}_1-\vec{R}_2)}\delta V_1(\vec{Q})\chi_B(\vec{Q})\delta V_2(\vec{Q})\ , \tag{29}$$

to the bulk pair potential has been removed. More appropriate is the rate of convergence of ϕ_s relative to the bulk pair potential ϕ_b ($\phi_b\equiv\phi_e+\phi_{\text{bare}}$). This is detailed in Figs. 8 and 9 for two atoms on the first and second planes of a (110) face of Al.

We note the very large changes in ϕ_b coming from ϕ_s (even in the second plane) and this persists at least two more planes into the metal. The convergence to ϕ_b is clearly very slow, and it is expected that modification to phonon frequencies (as an example) in all metals will persist for many planes. Note that the surface details (i.e., ψ) dominate the correction in the pair interaction, and we conclude that surface changes (e.g., due to adsorbates) *must* severely affect the force constants of the substrate and the corresponding surface phonon modes. In Fig. 10, we present the results of two different higher-order derivatives from the surface contribution to the pair potential[27] and compare them to the second derivative of the bulk pair interaction. These derivatives are directly related to the various force constants.[7] We find systematically that $\partial^2\phi_s/\partial z_1\partial z_2$ makes the largest change to the bulk force constants, and we expect the transverse surface phonon modes to exhibit a large sensitivity from surface screening. We do not include the force-constant changes from $\partial^2\phi_s/\partial\rho^2$ which we find are even smaller than $\partial^2\phi_s/\partial\rho\partial z_1$. The sensitivity to two choices of pseudopotential parameters are also demonstrated.

There are major changes in the qualitative structure of

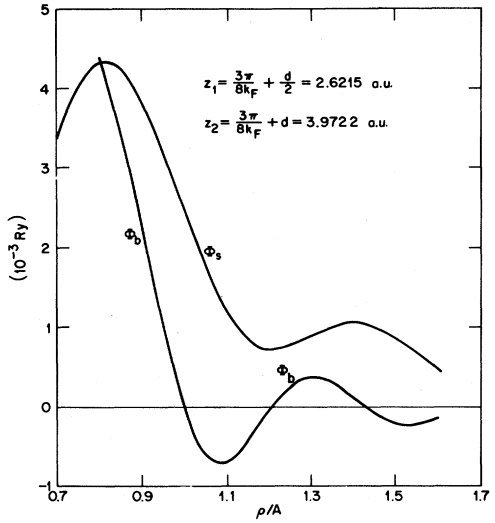

FIG. 11. Pair interaction for two Al pseudo ions: one placed in the first plane and the other in the second plane of an Al (110) face, as a function of separation. Exchange and correlation are included.

ϕ_b after the addition of ϕ_s (i.e., $\phi = \phi_s + \phi_b$). Most prominant is a shift in the location of the minimas and maximas which could at least partially account for reconstruction of some metallic faces. Figure 9 also clearly demonstrates the importance of including exchange and correlation effects in ϕ_s. In Fig. 11 we plot the pair potentials between atoms in the first and second planes. Note the resulting additional structure which would be hard to predict just from the two previous results of Figs. 8 and 9.

To produce reliable pair potentials for real metallic surfaces and for numerical applications of force-constant changes to the corresponding surface-phonon dispersions requires a formulation which accounts for the fine surface details discussed above. We are working on such considerations and on more accurate parametrization of the bulk density response (see Fig. 5).

ACKNOWLEDGMENTS

We wish to thank Dr. S. H. Liu for a critical reading of the manuscript. This research was sponsored by the Division of Materials Sciences, U.S. Department of Energy under Contract No. W-7405-ENG-26 with Union Carbide Corporation.

[1]For a perturbation $\delta V_1(\vec{r}-\vec{R}_1)$ of very long wavelength, this is no longer true and the perturbation expansion must be pursued to fourth order; see, E. G. Brovman and Y. Kagan, Zh. Eksp. Teor. Fiz. 57, 1329 (1969) [Sov. Phys.—JETP 30, 721 (1970)].

[2]D. L. Price, K. S. Singwi, and M. P. Tosi, Phys. Rev. B 2, 2983 (1980).

[3]W. E. Pickett, A. J. Freeman, and D. D. Koelling, Phys. Rev. B 22, 2695 (1980).

[4]A. Rahman, Phys. Rev. Lett. 32, 52 (1974).

[5]A. Fasolino, G. Santovo, and E. Tosatti, Phys. Rev. Lett. 44, 1684 (1980).

[6]J. E. Inglesfield, J. Phys. C 12, 149 (1979).

[7]M. Rasolt and M. Mostoller, Phys. Rev. B 23, 3774 (1981); Phys. Lett. 88A, 93 (1982).

[8]R. Evans and R. Kamaravadival, J. Phys. C 9, 1891 (1976).

[9]K. K. Mon and D. Stroud, Phys. Rev. Lett. 45, 817 (1980).

[10]J. F. Dobson and J. H. Rose, J. Phys. C 15, 7429 (1982).

[11]E. Tosatti and P. W. Anderson, Solid State Commun. 14, 773 (1974).

[12]P. J. Feibelman, Phys. Rev. B 12, 1319 (1975).

[13]W. Kohn and L. J. Sham, Phys. Rev. 140, A1133 (1965).

[14]The static susceptibility is a ground-state response; therefore, it is a functional of $n(\vec{r})$ and describable in terms of $\phi_k(\vec{r})$.

[15]M. Gell-Mann and K. A. Brueckner, Phys. Rev. 106, 364 (1957).

[16]We use for $\Pi_B(Q)$ the form of D. J. W. Geldart and R. Taylor, Can. J. Phys. 48, 155 (1970); 48, 167 (1970).

[17]D. M. Newns, Phys. Rev. B 1, 3304 (1970); D. C. Langreth and J. P. Perdew, *ibid.* 15, 2884 (1977).

[18]J. Hubbard, Proc. R. Soc. London 243, 336 (1957). We note that the Kohn-Sham approach to correlation does not account for the structure of the local-field corrections around $Q = 2k_F$; important to the pair interactions at long range.

[19]M. Rasolt and R. Taylor, Phys. Rev. B 11, 2717 (1975); L. Dagens, M. Rasolt, and R. Taylor, *ibid.* 11, 2726 (1975).

[20]J. S. Y. Wang and M. Rasolt, Phys. Rev. B 13, 5330 (1976).

[21]M. Rasolt, J. S. Y. Wang, and L. M. Kahn, Phys. Rev. B 15, 580 (1977).

[22]V. Sahni, J. B. Krieger, and J. Gruenebaum, Phys. Rev. B 15, 1941 (1977).

[23]D. E. Beck and V. Celli, Phys. Rev. B 2, 2955 (1970).

[24]L. M. Garrido, F. Flores, F. Garcia, and M. Oliner, J. Phys. F 9, 1097 (1979).

[25]N. D. Lang and W. Kohn, Phys. Rev. B 3, 1215 (1971).

[26]J. A. Appelbaum and D. R. Hamann, Phys. Rev. B 6, 1122 (1972).

[27]These derivatives were calculated by differentiating Eq. (15) with respect to z_1 and z_2. This of course requires the solution of Eq. (14) for a new set of related quantities.